

Research Article

Optimization of $\text{LaPO}_4:\text{Bi}^{3+}$ Single-Phased White-Emitting Phosphor Luminescence Properties by Li^+/Na^+ Doping

Taoli Deng  and Qiuyun Zhang 

School of Chemistry and Chemical Engineering, Anshun University, Anshun, 561000 Guizhou, China

Correspondence should be addressed to Taoli Deng; 708955582@qq.com and Qiuyun Zhang; sci_qy Zhang@126.com

Received 22 December 2018; Accepted 10 February 2019; Published 3 March 2019

Academic Editor: Sulaiman W. Harun

Copyright © 2019 Taoli Deng and Qiuyun Zhang. This is an open access article distributed under the Creative Commons Attribution License, which permits unrestricted use, distribution, and reproduction in any medium, provided the original work is properly cited.

$\text{LaPO}_4:\text{Bi}^{3+}$ single-phased white-emitting phosphors doped with both Li^+/Na^+ ions were successfully prepared by a conventional solid-state reaction technique. Microstructures were analyzed by both X-ray diffraction and high-resolution scanning electron microscopy experiments. Under the excitation of 335 nm, the $\text{La}_{0.97}\text{PO}_4:\text{Bi}^{3+}_{0.03}$ phosphor showed four emission bands with maxima at 460 nm, 487 nm (blue), 530 nm (yellow), and 637 nm (red); these can be successfully combined to form pure white light in a single host lattice only by simple activator Bi^{3+} ion. It was found that changing the concentration of dopant (Li^+ , Na^+ ions) did not produce a change in shape or location of the emission peaks, but the value of the emission intensity increased; this was particularly evident in the red emission, which could optimize the white light emitting performance of the phosphors. When the Na^+ doping concentration was 0.02, the CIE chromaticity coordinate of phosphor $\text{La}_{0.95}\text{PO}_4:\text{Bi}^{3+}_{0.03}, \text{Na}^+_{0.02}$ was (0.3008, 0.3203), close to that of the standard white light.

1. Introduction

In recent years, white light-emitting diodes (WLEDs) have attracted significant attention as a promising general illumination source, due to their small volume, low energy consumption, high luminous efficiency, good safety record, and long lifetime [1–3].

At present, there are two alternative approaches to WLED assembly. The main strategy in producing white light is to combine a blue LED chip with a YAG: Ce yellow phosphor. However, it is of note that several defects have been identified in this method. Firstly, blue light LEDs have low luminescence efficiency, and as device color is changed by a combination of the working temperature, voltage, and the phosphor coating thickness, this makes the white light emission unstable. Secondly, a lack of red light components results in white light which has both a high color temperature and poor color rendering index. An alternative approach in the generation of white light is to use the UV chip coated with blend of tri-chromatic phosphors, which is considered more competitive in terms of color uniformity, color rendition,

and long-term color stability. However, the blue emission efficiency is still poor in this white light LED system, due to the strong reabsorption of blue light by the green and red phosphors [4–7]. Therefore, the development of a series of single-phased white light phosphors is very important, which is with tunable emissions to enhance the luminous efficiency and color rendering index. It has been shown that nonrare trivalent bismuth (Bi^{3+}) can exhibit emission in UV, emitting in the blue, green, yellow, and red regions; depending on the susceptibility of the 6s electrons to the surrounding field [8], this results in a tunable emission band from the Bi^{3+} ions in various doped host phosphors [9–12].

LaPO_4 is an excellent phosphor host, exhibiting remarkable chemical and thermal stability, having a monoclinic structure, in a single crystallographic position (P 21/n group), which is available for trivalent ions [13]. Photoluminescence properties of LaPO_4 as the host material have been extensively researched in the literature [14–18]. Few single-component white-emitting phosphors codoping $\text{Bi}^{3+}/\text{Eu}^{3+}$ ions have been reported [19, 20]. However, the white-emitting phosphor $\text{LaPO}_4:\text{Bi}^{3+}$ of single host lattice only by simple

activator Bi^{3+} ion is a new research, in which the white light emitting performance can be optimized by Li^+/Na^+ doping.

2. Experimental

2.1. Sample Preparation. Powder samples $\text{La}_{0.97-x}\text{PO}_4:\text{Bi}^{3+}_{0.03}, \text{Li}^+_x$ ($x = 0.00, 0.01, 0.02, 0.03$) and $\text{La}_{0.97-y}\text{PO}_4:\text{Bi}^{3+}_{0.03}, \text{Na}^+_y$ ($y = 0.00, 0.01, 0.02, 0.03$) were synthesized by a conventional solid-state reaction technique [21]. Stoichiometric amounts of La_2O_3 (99.99%), Bi_2O_3 (99.99%), Li_2CO_3 (>99.0%), Na_2CO_3 (>99.0%), and $\text{NH}_4\text{H}_2\text{PO}_4$ (>99.0%) were thoroughly mixed and ground in an agate mortar, before addition of a 2% excess of $(\text{NH}_4)_2\text{HPO}_4$ to compensate for the evaporation of phosphorus species during high-temperature solid state reactions. The mixture was subsequently calcined successively in air at 800°C for 1 h and then at 1200°C for 8 h. After cooling to room temperature, the calcined samples were prepared for measurement by crushing

2.2. Characterization. The phase purity of the phosphors was checked by advance X-ray diffractometry (D/MAX-2200) with $\text{Cu K}\alpha$ radiation ($\lambda = 0.154056$ nm) operated at 40 mA and 40 kV. The phosphors morphology was investigated by scanning electron microscope (EGA 3 SBU). The photoluminescence excitation (PLE) and emission (PL) spectra of the phosphors were recorded using spectrofluorimetry (PE LS55) at room temperature.

3. Results and Discussion

3.1. Crystal Structure and Morphology Analysis. Figures 1 and 2 present the representative XRD patterns of the $\text{La}_{0.97-x-y}\text{PO}_4:\text{Bi}^{3+}_{0.03}, \text{Li}^+_x, \text{Na}^+_y$ ($x = 0.00, 0.01, 0.02, 0.03, y = 0.00, 0.01, 0.02, 0.03$) samples. Each phosphor spectral pattern has been successfully assigned and shows a match with standard data single phase for monoclinic LaPO_4 (JCPD#35-0731) [22], with no other impurities detected. This indicates that $\text{Bi}^{3+}, \text{Li}^+$, and Na^+ ions have been successfully incorporated into the LaPO_4 host lattices. When compared to the pattern of $\text{La}_{0.97}\text{PO}_4:\text{Bi}^{3+}_{0.03}$ phosphor, the spectral peaks of the phosphors have shifted to larger diffraction following Li^+ and Na^+ doping. This proves that Li^+ and Na^+ ions were incorporated into LaPO_4 host crystal, by substitution of the La^{3+} . Due to the fact that the ionic radii of Li^+ (0.076nm, CN=8) and Na^+ (0.102nm, CN=8) are smaller than that of La^{3+} (1.172 nm, CN=8) [23], incorporation of Li^+/Na^+ ions into LaPO_4 is observed, resulting in the contraction of the host lattice. When the concentration of Li^+ and Na^+ ions is increased to 0.03, the diffraction peaks no longer shift to larger diffraction, implying that dopant ions may now be in the interstitial position rather than substituting the lattice ions [24].

The average sizes of the crystallites were estimated by Scherrer's equation [25]:

$$D = \frac{0.89\lambda}{\beta \cos \theta} \quad (1)$$

where D is the average crystallite size, λ is the wavelength of the $\text{Cu K}\alpha$ line, θ is the Bragg angle, and β is the full-width at half maximum in radians. The strongest peak at 28.6° ($\beta=0.064$) was used to estimate the crystallite size by the Scherrer equation. Using this procedure gave an average crystallite size of 2.44 nm, for the prepared phosphor particles.

SEM analysis of $\text{La}_{0.97}\text{PO}_4:\text{Bi}^{3+}_{0.03}$ (Figure 3), calcined at 1200°C for 8 h, and then cooling to room temperature by crushing, indicates that the phosphors exhibit a quasi-spherical morphology with a size range of $0.5 \mu\text{m}$ - $1 \mu\text{m}$, with the prepared phosphor particles showing good dispersity.

3.2. PL and PLE Analysis. Figure 4 shows PL and PLE spectra of $\text{La}_{0.97}\text{PO}_4:\text{Bi}^{3+}_{0.03}$. By monitoring of the emission at 637 nm, the PLE spectrum shows a weak band with maxima at 380 nm and a strong band at 335 nm, respectively. The strong excitation peak belongs to the $^1\text{S}_0 \rightarrow ^3\text{P}_1$ transition of Bi^{3+} ions. The PL spectrum excited by 335 nm radiation shows four emission bands with maxima at 460 nm, 487 nm (blue), 530 nm (yellow), and 637 nm (red). Interestingly, the emission spectrum covers the entire visible region from 400 nm to 700 nm, and these three emission bands can be successfully combined to form pure white light, in the single host lattice containing a simple activator Bi^{3+} ion. As we know, the electronic configuration of trivalent bismuth (Bi^{3+}) is $[\text{Xe}]-4f^{14}5d^{10}6s^2$, its ground state is $^1\text{S}_0$, and the excited states of $6s$ $6p$ configuration in an increasing energy order can be split into $^3\text{P}_0, ^3\text{P}_1, ^3\text{P}_2$, and $^1\text{P}_1$ levels. The transitions of $^1\text{S}_0 \rightarrow ^3\text{P}_0$ and $^1\text{S}_0 \rightarrow ^3\text{P}_2$ are parity forbidden, but the transitions of $^1\text{S}_0 \rightarrow ^3\text{P}_1$ or $^1\text{P}_1$ are parity allowed due to spin orbit coupling [26]. According to the energy levels of Bi^{3+} , the red, yellow, and blue emissions are due to $^3\text{P}_1 \rightarrow ^1\text{S}_0$ transition depending on the susceptibility of its $6s$ electrons to the surrounding field.

3.3. Discussions on the Tunable Emissions. In order to optimize the white light emitting performance of the phosphors, a series of samples with different doping concentration of Li^+ and Na^+ were synthesized and their PL spectra were investigated. Figures 5 and 6 showed the emission spectra of phosphors $\text{La}_{0.97-x-y}\text{PO}_4:\text{Bi}^{3+}_{0.03}, \text{Li}^+_x, \text{Na}^+_y$ ($x = 0.00, 0.01, 0.02, 0.03, y = 0.00, 0.01, 0.02, 0.03$) and the emissions intensities at 487 nm (blue), 530 nm (yellow), and 637 nm (red) on Li^+ and Na^+ doping concentration. Figure 5(a) shows that the emission intensity at 637 nm is relatively unaffected by increasing Li^+ doping concentration and reached maximum intensity at $x=0.01$. Conversely, the emissions intensity at 487 nm and 530 nm increased slowly as shown in Figure 5(b).

A marked improvement in the emission spectra is observed when the Na^+ doping concentration is increased (Figure 6(a)); the red emission intensity at 637 nm increased significantly and reached the highest a dope concentration of 0.02, with the emissions intensity at 487 nm and 530 nm still being increased slowly as shown in Figure 6(b), which indicated that the intensity of red emission at 637 nm is strongly influenced by the surrounding environment around

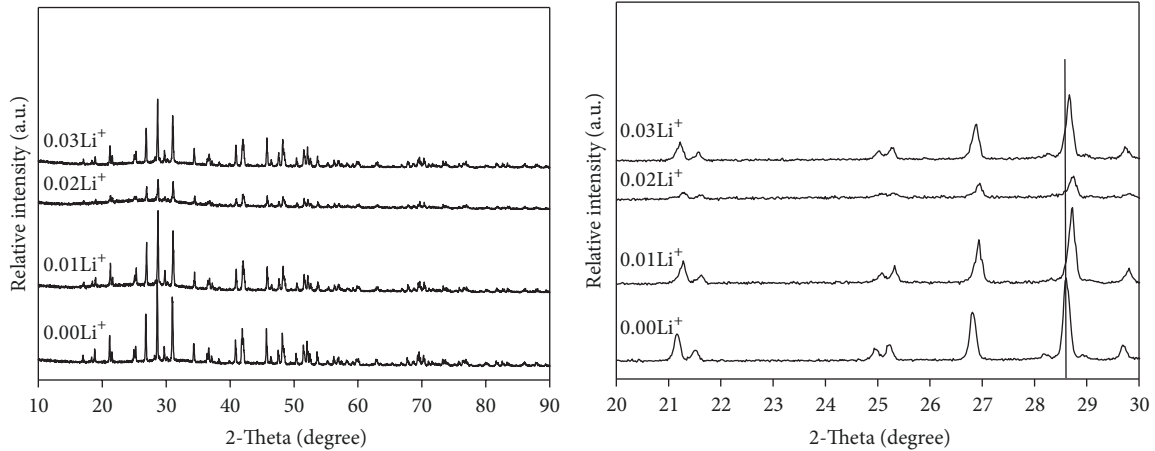


FIGURE 1: XRD patterns of $\text{La}_{0.97-x}\text{PO}_4:\text{Bi}^{3+}_{0.03}, \text{Li}^+_x$ ($x = 0.00, 0.01, 0.02, 0.03$) samples calcined at 1200°C for 8 h.

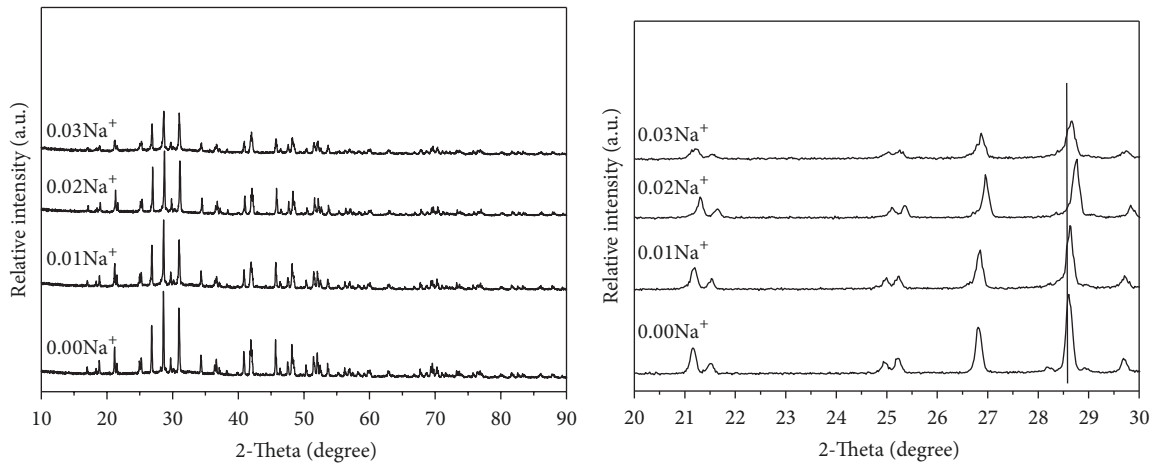


FIGURE 2: XRD patterns of $\text{La}_{0.97-y}\text{PO}_4:\text{Bi}^{3+}_{0.03}, \text{Na}^+_y$ ($y = 0.00, 0.01, 0.02, 0.03$) samples calcined at 1200°C for 8 h.

the Bi^{3+} . Since Li^+ and Na^+ ions were incorporated into the LaPO_4 host crystal, by substitution of the La^{3+} in the interstitial position of host crystal, reducing the symmetry of the matrix materials and favoring for release of the forbidden parity, and promoting the f-f electronic transitions, which in turn increases the intensity of the red emission. Meanwhile, doping of Li^+ and Na^+ ions creates a charge imbalance between the phosphor systems, enhancing the activity of oxygen vacancies which can be subsequently used as a sensitizer to transfer energy to rare earth luminescent ions via charge transfer, again increasing red emission intensity [27].

Different doping concentration of Li^+ and Na^+ ions does not produce a change in shape or location of the emission peaks, but the value of emission intensity changes especially for the red emission effecting a movement of the CIE coordinates (x, y). Table 1 shows the CIE coordinates (x, y) of various concentrations of the samples and correlated color temperature (CCT) and Figure 7 represents the corresponding CIE chromaticity diagram of the phosphors

$\text{LaPO}_4:\text{Bi}^{3+}$ by doping Li^+/Na^+ ions. All the CIE coordinates shown in Table 1 of the $\text{La}_{0.97-x-y}\text{PO}_4:\text{Bi}^{3+}_{0.03}, \text{Li}^+_x, \text{Na}^+_y$ ($x = 0.00, 0.01, 0.02, 0.03, y = 0.00, 0.01, 0.02, 0.03$) phosphors fall into the nearly white light region in the CIE diagram, which makes it suitable for the fabrication of white light emitting LEDs [28, 29].

It has been proven that the red emission intensity increases with the Li^+/Na^+ ions doping; then, changing Li^+/Na^+ ions concentrations can adjust the CIE and CCT. In $\text{La}_{0.97-x-y}\text{PO}_4:\text{Bi}^{3+}_{0.03}, \text{Li}^+_x, \text{Na}^+_y$ ($x = 0.00, 0.01, 0.02, 0.03, y = 0.00, 0.01, 0.02, 0.03$) phosphors by varying concentration of Li^+/Na^+ from 0 to 0.03 mol, the corresponding color tone shifted from the blue-green to white region as shown in Figure 6 (point a→b→c→d, a→e→f→g). When the Na^+ doping concentration is 0.02, the CIE chromaticity coordinates of phosphor $\text{La}_{0.95}\text{PO}_4:\text{Bi}^{3+}_{0.03}, \text{Na}^+_{0.02}$ are (0.3008, 0.3203), close to that of the standard white light. Low CCT value implies warmer light, while the high CCT indicates colder tones [30]. For all the prepared phosphor samples, the CCT values are found to be above

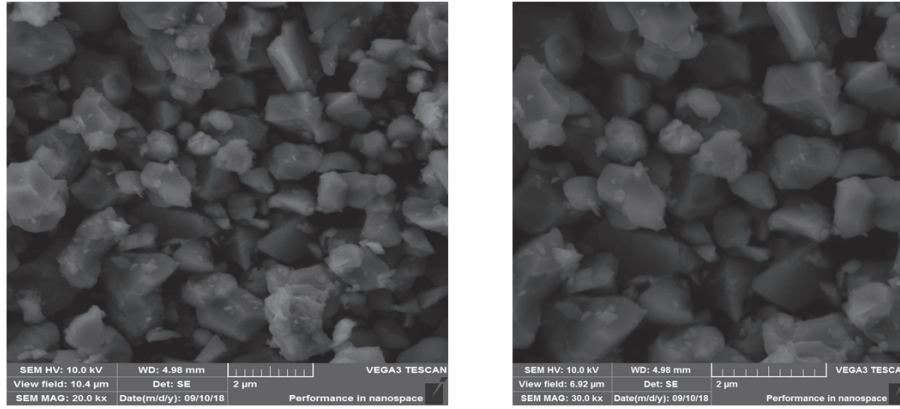


FIGURE 3: SEM images of $\text{La}_{0.97}\text{PO}_4:\text{Bi}^{3+}_{0.03}$ samples after calcination at 1200°C for 8 h.

TABLE 1: The color coordinates of various color concentrations of the samples and correlated color temperature.

Samples	CIE coordinates (x,y)	CCTs
$\text{La}_{0.97}\text{PO}_4:0.03\text{Bi}^{3+}$ (a)	(0.2778, 0.3278)	8708k
$\text{La}_{0.96}\text{PO}_4:0.03\text{Bi}^{3+}, 0.01\text{Li}^+$ (b)	(0.2956, 0.3221)	7520K
$\text{La}_{0.95}\text{PO}_4:0.03\text{Bi}^{3+}, 0.02\text{Li}^+$ (c)	(0.2775, 0.3280)	8725K
$\text{La}_{0.94}\text{PO}_4:0.03\text{Bi}^{3+}, 0.03\text{Li}^+$ (d)	(0.2798, 0.3226)	8699K
$\text{La}_{0.96}\text{PO}_4:0.03\text{Bi}^{3+}, 0.01\text{Na}^+$ (e)	(0.2821, 0.3228)	8528K
$\text{La}_{0.95}\text{PO}_4:0.03\text{Bi}^{3+}, 0.02\text{Na}^+$ (f)	(0.3008, 0.3203)	7302K
$\text{La}_{0.94}\text{PO}_4:0.03\text{Bi}^{3+}, 0.03\text{Na}^+$ (g)	(0.2797, 0.3252)	8640K

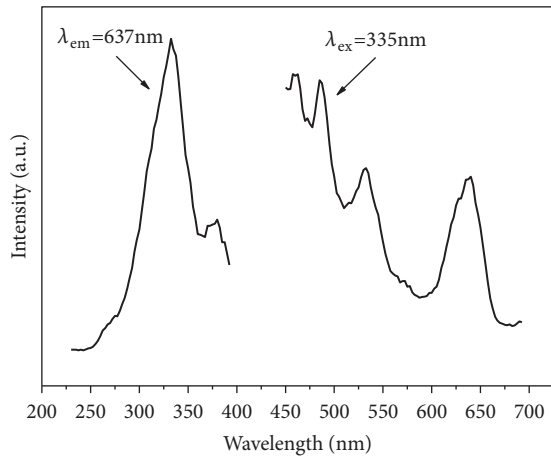


FIGURE 4: PL and PLE spectra of $\text{La}_{0.97}\text{PO}_4:\text{Bi}^{3+}_{0.03}$ phosphor.

5000 K, which can be regarded as a cool white light for commercial applications [31].

4. Conclusions

The luminescence properties of $\text{LaPO}_4:\text{Bi}^{3+}$ single-phased white-emitting phosphors were optimized by Li^+/Na^+ doping, prepared by conventional solid-state reaction techniques. The prepared phosphor particles show good dispersity with a size range of $0.5\mu\text{m}$ - $1\mu\text{m}$. It was found that the PL spectrum excited by 335 nm radiation shows four emission bands with

maxima at 460 nm, 487 nm (blue), 530 nm (yellow), and 637 nm (red), covering the entire visible region from 400 nm to 700 nm. These color emission bands can be successfully combined to form pure white light in the single host lattice only by simple activator Bi^{3+} ion. The phosphor emission intensity at 637 nm hardly increases with Li^+ and Na^+ doping, making the corresponding color tone shifted from the blue-green to white region. Finally, for the $\text{LaPO}_4:\text{Bi}^{3+}$ single-phased phosphors optimized by doping with Li^+/Na^+ when the Na^+ doping concentration is 0.02, the CIE chromaticity coordinates is (0.3008, 0.3203), which has been close to that of the standard white light, and can be regarded as a cool white light for commercial applications.

Data Availability

The data used to support the findings of this study are available from the corresponding author upon request.

Conflicts of Interest

The authors declare that they have no conflicts of interest.

Acknowledgments

This work was financially supported by the Youth Growth S&T Personnel Foundation of Guizhou Education Department (KY [2016]273, KY [2017]283), the Joint Science and Technology Funds of Guizhou S&T Department, Anshun

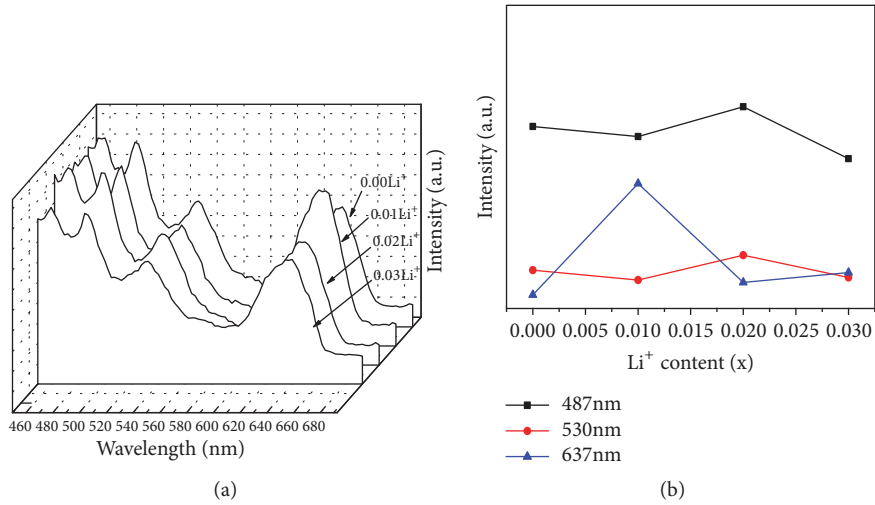


FIGURE 5: Emission spectra ($\lambda_{\text{ex}}=335\text{nm}$) of $\text{La}_{0.97-x}\text{PO}_4:\text{Bi}^{3+}, \text{Li}^+_x$ ($x = 0.00, 0.01, 0.02, 0.03$) phosphors (a). The emissions intensity of 487 nm (blue), 530 nm (yellow), and 637 nm (red) as function of Li^+ doping concentration (red) (b).

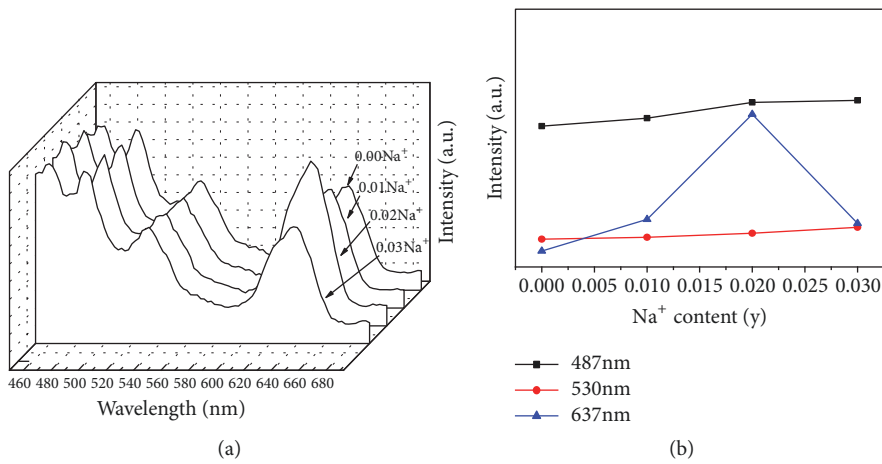


FIGURE 6: Emission spectra ($\lambda_{\text{ex}} = 335\text{nm}$) of $\text{La}_{0.97-y}\text{PO}_4:\text{Bi}^{3+}, \text{Na}^+_y$ ($y=0.00, 0.01, 0.02, 0.03$) phosphors (a). The emissions intensity of 487 nm (blue), 530 nm (yellow), and 637 nm (red) as function of Na^+ doping concentration (red) (b).

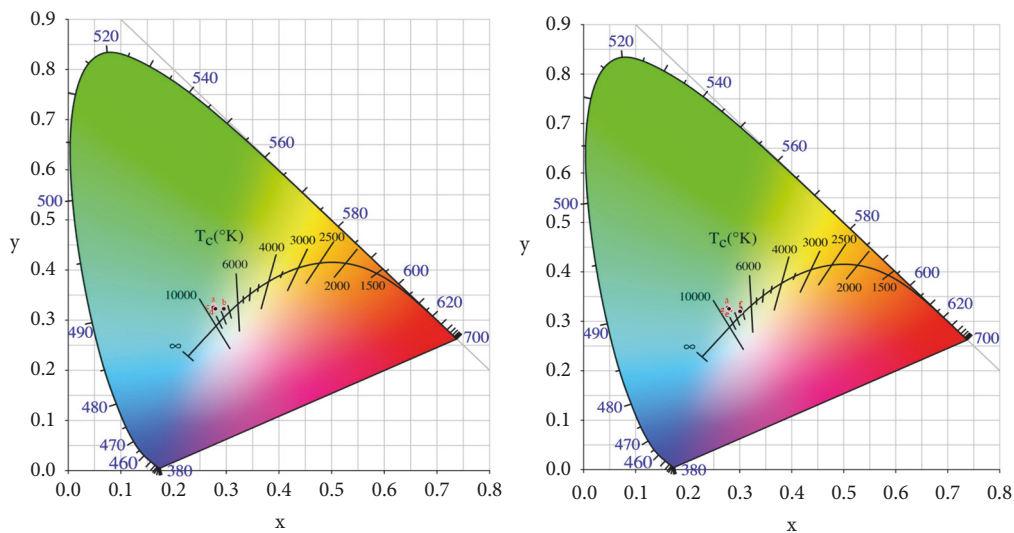
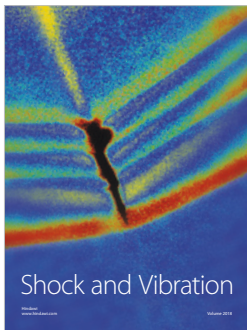
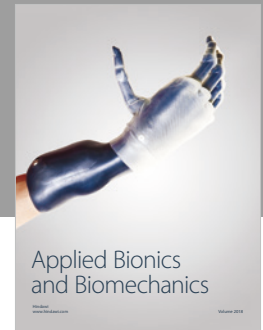
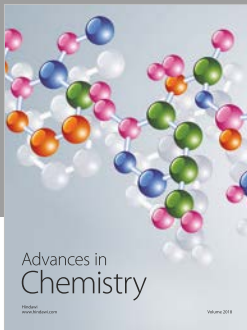


FIGURE 7: CIE chromaticity coordinates of $\text{La}_{0.97-x-y}\text{PO}_4:\text{Bi}^{3+}, \text{Li}^+_x, \text{Na}^+_y$ ($x = 0.00, 0.01, 0.02, 0.03, y = 0.00, 0.01, 0.02, 0.03$) phosphors.

City People's Government, and Anshun University (LH [2016]7271).

References

- [1] J. S. Kim, P. E. Jeon, Y. H. Park et al., "White-light generation through ultraviolet-emitting diode and white-emitting phosphor," *Applied Physics Letters*, vol. 85, no. 17, pp. 3696–3698, 2004.
- [2] N. Guo, Y. Huang, H. You et al., "Ca₉Lu(PO₄)₇:Eu²⁺,Mn²⁺: A Potential Single-Phased White-Light-Emitting Phosphor Suitable for White-Light-Emitting Diodes," *Inorganic Chemistry*, vol. 49, pp. 10907–10913, 2010.
- [3] X. Huang and H. Guo, "LiCa₃MgV₃O₁₂:Sm³⁺: A new high-efficiency white-emitting phosphor," *Ceramics International*, vol. 44, no. 9, pp. 10340–10344, 2018 (Catalan).
- [4] F. Kang, M. Peng, X. Yang, and J. Mater, "Broadly tuning Bi³⁺ emission via crystal field modulation in solid solution compounds (Y,Lu,Sc)VO₄:Bi for ultraviolet converted white LEDs," *Journal of Materials Chemistry C*, vol. 2, pp. 6068–6076, 2014.
- [5] H. H. Yu, M. Y. Zhao, L. J. Qu et al., "Synthesis and spectral properties of BaWO₄:Eu³⁺ phosphors for white light emitting diodes," *Journal of Synthetic Crystals*, vol. 46, pp. 38–42, 2017.
- [6] W. J. Jin, Y. Kim, O. H. Kwon, and S. C. Yong, "Flexible micro-scale UV-curable phosphor layers screen-printed on a polymer substrate for planar white light-emitting diodes," *Materials Letters*, vol. 217, pp. 124–126, 2018.
- [7] W. J. Jin, Y. Kim, O. H. Kwon, T. H. Lee, and S. C. Yong, "UV-curable silicate phosphor planar films printed on glass substrate for white light-emitting diodes," *Optics Letters*, vol. 40, pp. 3723–3726, 2015.
- [8] H. H. Zhou, "Temperature dependence of energy transfer in tunable white light-emitting phosphor BaY₂Si₃O₁₀:Bi³⁺,Eu³⁺ for near UV LEDs," *Journal of Materials Chemistry C*, vol. 3, pp. 11151–11162, 2015.
- [9] F. Kang, X. Yang, M. Peng et al., "Red photoluminescence from Bi³⁺ and the influence of the oxygen-vacancy perturbation in ScVO₄: a combined experimental and theoretical study," *The Journal of Physical Chemistry C*, vol. 118, pp. 7515–7522, 2014.
- [10] D. Chen, Y. Yu, P. Huang, H. Lin, Z. Shan, and L. Zeng, "Color-tunable luminescence for Bi³⁺/Ln³⁺:YVO₄ (Ln = Eu, Sm, Dy, Ho) nanophosphors excitable by near-ultraviolet light," *Physical Chemistry Chemical Physics*, vol. 12, pp. 7775–7778, 2010.
- [11] M. Nikl, A. Novoselov, E. Mihoková et al., "Photoluminescence of Bi³⁺ in Y₃Ga₅O₁₂ single-crystal host," *Journal of Physics: Condensed Matter*, vol. 17, no. 21, pp. 3367–3375, 2005.
- [12] J. Han, F. Pan, M. S. Molokeev et al., "Redefinition of crystal structure and Bi³⁺ yellow luminescence with strong near-ultraviolet excitation in La³BWO⁹:Bi³⁺ phosphor for white light-emitting diodes," *ACS Applied Materials & Interfaces*, vol. 10, pp. 13660–13668, 2018.
- [13] A. A. Ansari, "Silica-modified luminescent LaPO₄:Eu@LaPO₄@SiO₂ core/shell nanorods: synthesis, structural and luminescent properties," *Luminescence*, vol. 33, no. 1, pp. 112–118, 2017.
- [14] G. Bühler and C. Feldmann, "Microwave-assisted synthesis of luminescent LaPO₄:Ce,Tb nanocrystals in ionic liquids," *Angewandte Chemie International Edition*, vol. 45, no. 29, pp. 4865–4867, 2006.
- [15] S. Ray, G. B. Nair, P. Tadge et al., "Size and shape-tailored hydrothermal synthesis and characterization of nanocrystalline LaPO₄:Eu³⁺ phosphor," *Journal of Luminescence*, vol. 194, pp. 64–71, 2018.
- [16] N. P. Shaik, N. V. Poornachandra Rao, and K. V. R. Murthy, "Synthesis and photoluminescent properties of LaPO₄:Ga³⁺ phosphor," *Archives of Physics Research*, vol. 5, pp. 45–49, 2014.
- [17] Y. F. Han, W. Ying, G. X. Li, F. S. Pan, R. H. Fan, and X. F. Liu, "Effect of Sm³⁺ concentration on the vibrational and luminescent properties of LaPO₄," *Materials Science Forum*, vol. 848, pp. 482–488, 2016.
- [18] T. S. Malyy, V. V. Vistovskyy, and Z. A. Khapko, "Recombination luminescence of LaPO₄," *Journal of Applied Physics*, vol. 113, no. 22, 2013.
- [19] K. Li, J. Fan, M. M. Shang, and H. Z. Lian, "Sr₂Y₈(SiO₄)₆O₂:Bi³⁺/Eu³⁺: a single-component white-emitting phosphor via energy transfer for UV w-LEDs," *Journal of Materials Chemistry C*, vol. 3, pp. 9989–9998, 2015.
- [20] Z. Jiang, X. Yu, J. Gou et al., "Design, luminescence and energy transfer of single-phased color-tunable YNbO₄:Bi³⁺,Eu³⁺ phosphor for UV pumped white light-emitting diodes," *Journal of Materials Science: Materials in Electronics*, vol. 28, no. 4, pp. 3630–3636, 2017.
- [21] T. L. Deng, S. R. Yan, and J. G. Hu, "A novel narrow band UV-B emitting phosphor-YPO₄:Sb³⁺,Gd³⁺," *Journal of Rare Earths*, vol. 34, pp. 137–142, 2016.
- [22] X. Huang, "Preparation and luminescence characteristics of monazite Eu³⁺:LaPO₄ nanocrystals in NH₄NO₃ molten salt," *Optical Materials*, vol. 50, pp. 81–86, 2015.
- [23] H. Liu, Y. Hao, J. Wang, P. Zhao, P. Huang, and B. Xu, "Luminescent properties of R⁺ doped Sr₂SiO₄:Eu³⁺ (R⁺=Li⁺, Na⁺ and K⁺) red-emitting phosphors for white LEDs," *Lumin*, vol. 131, pp. 2422–2426, 2011.
- [24] P. P. Liu, J. Yin, X. Y. Mi, L. X. Zhang, and L. Bie, "Enhanced photoluminescence of CaTiO₃:Eu³⁺ red phosphors prepared by H₃BO₃ assisted solid state synthesis," *Journal of Rare Earths*, vol. 31, no. 6, pp. 555–558, 2013.
- [25] A. L. Patterson, "The scherrer formula for X-ray particle size determination," *Physical Review A: Atomic, Molecular and Optical Physics*, vol. 56, no. 10, pp. 978–982, 1939.
- [26] F. Kang, X. Yang, and M. Peng, "Red photoluminescence from Bi³⁺ and the influence of the oxygen-vacancy perturbation in ScVO₄: a combined experimental and theoretical study," *Journal of Physical Chemistry C*, vol. 118, pp. 7515–7522, 2014.
- [27] T. L. Deng and X. B. Jiang, "Comparison of the up-conversion photoluminescence for GAP, GAG and GAM phosphors," *Optical Materials*, vol. 78, pp. 27–34, 2018.
- [28] M. S. Mendhe, S. P. Puppallwar, and S. J. Dhoble, "Novel single-component CaLaAlO₄:Tb³⁺, Eu³⁺ phosphor for white light-emission," *Optical Materials*, vol. 82, pp. 47–55, 2018.
- [29] M. Ferhi, S. Toumi, K. Horchani-Naifer, and M. Ferid, "Single phase GdPO₄:Dy³⁺ microspheres blue, yellow and white light emitting phosphor," *Journal of Alloys and Compounds*, vol. 714, pp. 144–153, 2017.
- [30] E. Sreeja, V. Vidyadharan, and S. K. Jose, "A single-phase white light emitting Pr³⁺ doped Ba₂CaWO₆ phosphor: synthesis, photoluminescence and optical properties," *Optical Materials*, vol. 78, pp. 52–62, 2018.
- [31] W. A. Dar, Z. Ahmed, K. Iftikhar, and J. Photoch, "Cool white light emission from the yellow and blue emission bands of the Dy(III) complex under UV-excitation," *Journal of Photochemistry and Photobiology A: Chemistry*, vol. 356, pp. 502–511, 2018.



Hindawi

Submit your manuscripts at
www.hindawi.com

